

Kinematically Induced Dipole Anisotropy in Line-Emitting Galaxy Number Counts and Line Intensity Maps

Kyungjin Ahn

Department of Earth Sciences, Chosun University, Gwangju, 61452,
Korea.

Corresponding author(s). E-mail(s): kjahn@chosun.ac.kr;

Abstract

The motion of the solar system against an isotropic radiation background, such as the cosmic microwave background, induces a dipole anisotropy in the background due to the Doppler effect. Flux-limited observation of the continuum radiation from galaxies also has been studied extensively to show a dipole anisotropy due to the Doppler effect and the aberration effect. We show that a similar dipole anisotropy exists in spectral-line intensity maps, represented as either galaxy number counts or the diffuse intensity maps. The amplitude of these dipole anisotropies is determined by not only the solar velocity against the large-scale structures but also the temporal evolution of the monopole (sky-average) component. Measuring the dipole at multiple frequencies, which have mutually independent origins due to their occurrence from multiple redshifts, can provide a very accurate measure of the solar velocity thanks to the redundant information. We find that such a measurement can even constrain astrophysical parameters in the nearby universe. We explore the potential for dipole measurement of existing and upcoming surveys, and conclude that the spectral number count of galaxies through SPHEREx will be optimal for the first measurement of the dipole anisotropy in the spectral-line galaxy distribution. LIM surveys with reasonable accuracy are also found to be promising. We also discuss whether these experiments might reveal a peculiar nature of our local universe, that seems to call for a non-standard cosmology other than the simple Λ CDM model as suggested by recent measures of the baryon acoustic oscillation signatures and the Alcock-Paczynski tests.

Keywords: Cosmology, Cosmic microwave background, Dark energy, Sky Surveys

1 Introduction

Among the anisotropic modes in one of the most studied continuum foregrounds, the cosmic microwave background (CMB), the dipole anisotropy stands out in terms of its different origin from the rest (quadrupole and higher-order multipoles). The dipole anisotropy of the CMB in temperature is about 1.23×10^{-3} of the monopole value (2.725K), and thus is the largest of all the multipoles of the CMB anisotropy that, except for the dipole moment, range at $\lesssim 10^{-5}$ of the monopole. Such a largeness of the dipole anisotropy relative to other multipoles indicates that the dipole has a different origin, which is believed to be caused by the relative velocity of the observer (solar system) against the rest frame of CMB. It is thus natural to ignore the intrinsic dipole anisotropy due to the fluctuation in structure formation but instead fully attribute the CMB dipole to the kinematic origin and estimate the solar velocity v_{\odot} in units of c , $\beta_{\odot} \equiv v_{\odot}/c = (1.23 \pm 0.017) \times 10^{-3}$, against the CMB-rest frame. Of course the intrinsic dipole anisotropy must exist, and may be separated out if its small impact on the spectra of the monopole and quadrupole moments can be detected [1].

Dipole anisotropy exists also in the number distribution of continuum-emitting radiation sources, if observed with a fixed flux limit. Such a dipole must arise from the same kinematic origin, because the Doppler effect boosts the flux of galaxies toward the direction of the solar motion and thus increases the number of galaxies detected above a given flux limit. In addition, the light aberration also contributes to the dipole because galaxies will look more clustered toward the direction of motion than the opposite direction. This phenomenon was first formulated by [2], who worked on the case when continuum radiation from galaxies had a power-law flux $F \propto \nu^{-\alpha}$ and so does the number density, $N(> F) \propto F^{-x}$, to find that the amplitude of the dipole (D) becomes $D = [2 + x(1 + \alpha)]\beta_{\odot}$. Subsequently, actual observations of the dipole anisotropies in the number density of continuum-emitting galaxies [3–5] and quasars [6] followed to find that the estimated β_{\odot} is ~ 2 –5 times as high as that deduced from the CMB dipole, which is a very puzzling conflict for a single quantity. This conflict is considered by some as one of the non-negligible “tensions” between the standard cosmological model and observations, which mostly reside in the local universe of the line-of-sight comoving distance $\lesssim 3$ Gpc or $z \lesssim 1$ [7, 8].

There are about three categories of resolutions to this apparent paradox. First, systematic uncertainties arising from observations themselves are to blame. Re-analysis of the continuum galaxy data of the WISE (Wide-field Infrared Survey Explorer) survey resulted in β_{\odot} estimation statistically consistent with the CMB-based one [9], in contrast to the same WISE-based analysis undertaken previously [6], attributing the conflict to the systematic uncertainty caused by the observing and data-collecting schemes in WISE. However, the trend of estimated β_{\odot} from galaxy counts being different from the CMB-based estimation seems still persistent [10]. Even the direction of the dipole is in conflict, and thus some physical origin other than the kinematic origin may be responsible. Second, there may be an additional contribution to the dipole anisotropy from the biased structure formation. As suggested by [11], a high level of galaxy bias of ~ 3 could significantly boost the galaxy formation in high-density region, which is also a gravitational attractor driving the solar motion. However, the directional discrepancy between the galaxy number dipole and the CMB dipole (e.g.

[10]) seems to invalidate such claim. Third, one could explain such a discrepancy by adopting a non-standard cosmology with an anomalous universe. Then, one could have the CMB-rest frame in a relative motion against the matter-rest frame, resulting in mismatching dipole anisotropies probed by the CMB and the matter-density probes, namely galaxies [12].

Faced with the puzzle, more independent measures of similar dipole anisotropies seem necessary. Here we suggest using spectroscopic galaxy surveys (SGS) and line intensity mappings (LIM) to obtain their dipole anisotropy. To our knowledge, no such studies have been conducted to date, neither in theory or in observation. The SGS is to construct 3-dimensional galaxy maps from discrete, individually identifiable sources with redshift indicators such as a spectral line. The LIM is to construct 3-dimensional intensity maps from sources that are not identifiable — protogalaxies, galaxies and the intergalactic medium — by a telescope but collectively forming a diffuse background. However, so far all such surveys are either limited in the sky coverage, or aiming at the full sky but without spectroscopic capabilities. The only full-sky spectroscopic survey is SPHEREx (Spectro-Photometer for the History of the Universe, Epoch of Reionization, and Ices Explorer, [13]), which will be launched in the near future. In the dipole measurement, SGS and LIM can be more beneficial than the continuum-galaxy mapping because one could obtain true redundancy in estimating β_{\odot} by probing multiple redshifts through multiple observing frequencies. In contrast, even though the continuum-galaxy mapping has multi-frequency information, the amplitude of the continuum spectrum at any given frequency is an integral of multi-redshift contributions and thus lacks the distinctiveness of origin (and the corresponding redundancy) seen in line-galaxy surveys and LIMs. For example, huge radio interferometers have been in operation or are being built to map the intensity of the hydrogen 21-cm line (e.g. LOFAR (LOW Frequency ARray): [14], SKA-LOW (Square Kilometre Array – Low frequency): [15, 16]), either from very high redshifts ($z \gtrsim 6$ or the observing frequency $\nu \lesssim 200$ MHz) or from relatively low redshifts ($0 \leq z \lesssim 6$ or $200 \text{ MHz} \lesssim \nu \leq 1.4 \text{ GHz}$). We have elsewhere forecasted observations of the large-angle anisotropy of 21-cm lines: the dipole anisotropy [17] and the integrated Sachs-Wolfe effect [18] in the 21-cm background, both being the largest-angle (solid angle $\gtrsim (20^\circ)^2$) phenomena and thus requiring almost full-sky LIMs. We intend to extend and generalize our study of the 21-cm dipole anisotropy to the SGS and LIM dipoles.

This paper is organized as follows. In Sect. 2, we calculate the amplitude of the dipole anisotropy in SGS and LIM. In Sect. 3, we perform forecasting possible observations of SGS and LIM dipoles. Sect. 4 is dedicated to a brief summary and the discussion on the prospects of these proposed observations, with an emphasis on a serendipitous case when the estimated solar velocity happens to be found inconsistent with the value estimated by the CMB dipole measurement.

2 Theory

2.1 Notations and basic relations

We start from the cosmological principle asserting that the universe is homogeneous and isotropic in largest scales. The dipole anisotropy is of course the largest-scale

anisotropy, and thus is the case this principle suits best. We then need to introduce two different reference frames: (1) the background-rest frame (BRF) and (2) the observer-rest frame (ORF). The BRF denotes a frame in which the observer is comoving with the expansion of the universe, and to this observer the universe seems isotropic including any radiation background. The ORF denotes a frame attached to the solar system having us as the observer, and as described in Sect. 1 a radiation background will show the kinematically induced anisotropy.

We adopt a convention in which any scalar quantity A and vector quantity \mathbf{a} will be denoted without a prime in BRF while with a prime in ORF (A' and \mathbf{a}'). For example, F_ν represents the (true) differential flux at the observing frequency ν for an observer in BRF, while F'_ν represents the (apparent) differential flux at the observing frequency ν' for an observer in ORF. A quantity in one frame with an argument in another can also be defined: e.g. $F_{\nu'}$ represents the (true) differential flux but measured at ν' by an observer in ORF. Such a convention is a common practice especially in the literature of the kinematically induced anisotropy (e.g. [17, 19]). And we use the “apparent” cosmological redshift z' in ORF measured through spectroscopy of a line, such that $1 + z' = \nu_0/\nu'_c$ if the measured line center is at frequency ν'_c . From this point on, we assume all measurements are made at fixed z' (and with a fixed set of bandwidths) regardless of the line-of-sight direction \hat{n}' . Due to the smallness of β_\odot , one can expand the observed field in multipoles with ORF quantities in decreasing order, and up to the dipole we denote

$$A'(z', \hat{n}') = A'(z') + A'_{\text{dip}}\mu' = A(z') + A'_{\text{dip}}\mu', \quad (1)$$

where $\mu' \equiv \cos\theta'$ with the azimuthal angle θ against the direction of the observer’s motion, and $A'(z') = A(z')$ is the monopole component due to sources at redshift z' ¹.

Lorentz transformation gives the following conversion rules between quantities in BRF and those in ORF [17, 19, 21]:

$$\begin{aligned} \mu' &= \frac{\mu + \beta}{1 + \beta\mu} \\ \frac{\nu'}{\nu} &= \frac{d\nu'}{d\nu} = \frac{1}{\gamma(1 - \beta\mu')}, \\ \frac{dt'}{dt} &= \gamma(1 - \beta\mu'), \\ \frac{d\Omega'}{d\Omega} &= \gamma^2(1 - \beta\mu')^2, \\ \frac{F'}{F} &= \frac{dF'}{dF} = \frac{1}{\gamma^2(1 - \beta\mu')^2}, \end{aligned} \quad (2)$$

where β is the velocity (in units of c) of the observer against BRF, dt' is the photon arrival interval (thus the extra $1 - \beta\mu'$ in addition to the time dilation factor $\gamma = (1 - \beta^2)^{-1/2}$: [21] pp. 141), F is the bolometric flux of a line from a point source (e.g.

¹There exists $\mathcal{O}(\beta_\odot^2)$ correction on the monopole component in ORF [17, 20], due to the bleeding of the monopole into other multipoles. However, this correction is small and thus validates Eq. (1) up to $\mathcal{O}(\beta_\odot)$.

galaxy) such that $F_\nu \equiv dF/d\nu = F\phi(\nu)$ with the intrinsic line profile ϕ ($\int \phi(\nu) d\nu = 1$, and we assume $\phi(\nu) \simeq \delta(\nu - \nu_0)$ with the Dirac delta function δ without losing much generality throughout this paper), $d\Omega$ is the infinitesimal solid angle along the line-of-sight direction \hat{n} . For a source residing at cosmological redshift z , the redshifted line center is at $\nu_c = \nu_0/(1+z)$, while an ORF observer will have a shifted redshift z' satisfying

$$\begin{aligned} \nu'_c &= \nu_0/(1+z'), \\ 1+z' &= \gamma(1-\beta\mu')(1+z) \end{aligned} \quad (3)$$

even though it is not too common a practice to correct the observed redshift z' with Eq. (3).

2.2 Dipole anisotropy in galaxy number count

We construct a monopole “field” out of the point sources which are presumed to be isotropic in distribution and with universal physical quantities at a given redshift, for a comoving observer. The sources are assumed to have redshift indicators, or at least one spectral line. For a specific line emission (e.g. HI Ly α), we can again define the bolometric line flux F as $F_\nu = F\phi(\nu)$. Hereafter, F denotes this bolometric line flux.

The number density of line-emitting sources will bear a dipole anisotropy as follows. Suppose, in BRF, there are total N galaxies in the frequency range $\nu = [\nu_{\min}, \nu_{\max}]$ and the flux range $F = [F_{\min}, F_{\max}]$. Note that the observing frequency ν corresponds to the cosmological redshift z , and thus galaxies observed within some frequency range are those residing in the corresponding redshift range. Then, we can define the (differential) number density (galaxy number per unit frequency, flux and solid angle) as

$$n(F, \nu) = \frac{dN}{d\nu dF d\Omega}, \quad (4)$$

where we assumed isotropy in BRF and thus n does not have dependence on \hat{n}^2 . From now on, we assume that the universe is isotropic in BRF for the sake of calculating the kinematic dipole anisotropy. Even after the Lorentz transformation, the Lagrangian number should be conserved, or $dN' = dN$, satisfying

$$n'(F', \nu', \hat{n}') = n(F, \nu) \frac{d\nu}{d\nu'} \frac{dF}{dF'} \frac{d\Omega}{d\Omega'} = n(F, \nu) \gamma(1-\beta\mu'), \quad (5)$$

where the final relation is due to Eq. (2). After Taylor-expanding $n(F, \nu)$ in terms of the ORF parameters F' and ν' in Eq. (5), and using Eq. (3), we obtain the dipole moment of n' :

$$n'_{\text{dip}}(F', \nu') = -n(F', \nu') \left(1 + 2 \left. \frac{\partial \ln n}{\partial \ln F} \right|_{F', \nu'} + \left. \frac{\partial \ln n}{\partial \ln \nu} \right|_{F', \nu'} \right) \beta. \quad (6)$$

²If wanted, one can always use a new quantity $n(F, z) \equiv dN/dz dF d\Omega = n(F, \nu)(1+z)/\nu$.

In practice, one might want to use the cumulative number density

$$\mathcal{N}(\nu) \equiv \frac{dN}{d\nu d\Omega} = \int dF n(F, \nu). \quad (7)$$

This would be useful when the number of objects probed by a survey is not large enough to reliably construct n' , and thus it becomes necessary to mitigate the shot noise. Using the fact that $dN' = dN$ or $\mathcal{N}'(\nu', \hat{n}) d\Omega' d\nu' = \mathcal{N}(\nu) d\Omega d\nu$ with the help of Eq. (2), we find that

$$\mathcal{N}'_{\text{dip}}(\nu') = \mathcal{N}(\nu') \left(1 - \left. \frac{\partial \ln \mathcal{N}}{\partial \ln \nu} \right|_{\nu'} \right) \beta. \quad (8)$$

There are pros and cons in using n' and \mathcal{N}' for the dipole measurement. If we use n' , the dipole depends on F' which is of the astrophysical origin such as the mass-to-light ratio of cosmological halos, star formation rate, black-hole formation rate, etc. Therefore, the dipole of n' will bear astrophysical information just as the monopole of n' , in addition to the information on β_{\odot} . However, this will be realized only when the number of galaxies probed is large enough to span some flux range, because otherwise the statistical uncertainty from the shot noise might dominate the true signal. If we instead use \mathcal{N}' , the required number of objects to probe would not be as severe as for n' . However, the astrophysical information will be only limited to the cumulative number in frequency bins, or equivalently redshift bins, and thus the information content will be more limited. Nevertheless, as long as our interest lies only in probing β_{\odot} , the dipole of \mathcal{N}' could provide multiple frequency observables to constrain β_{\odot} . We show in Sect. 3.1 our forecast that can be used as a guide to future galaxy surveys.

Note that the derivation of Eqs. (6) and (8) are almost identical to that by Ref. [7] in that the calculation is based off the Lagrangian conservation of the number count across the BRF and the ORF. The difference lies in the fact that our derivation is for line emission but that by Ref. [7] is for continuum emission.

2.3 Dipole anisotropy in line intensity map

Line intensity maps at a certain observing frequency ν is associated with a collection of lines emitted (or absorbed, such as the Ly α forest) by various astrophysical objects at the cosmological redshift z satisfying $\nu = \nu_0/(1+z)$ with the line central frequency ν_0 . In BRF, the specific intensity (net energy per observed frequency, time, area and solid angle) is given by the cosmological radiative transfer equation,

$$I_{\nu} = \int ds'' \frac{j_{\nu''}(z'')}{(1+z'')^3}, \quad (9)$$

where ds is the light-of-sight distance travelled by a photon, $j_{\nu} \equiv dE/dV d\Omega dt d\nu$ with the energy E and the *proper* volume V , is the *proper* monochromatic emission coefficient ([21], pp. 9) in the source-rest frame, and the factor $1/(1+z)^3$ arises from the effect of the cosmological redshift on the observable (e.g. [22], Eq. 3.88). The absorption of a line by any gas in between the source and the observer, either in

BRF or ORF, does not exist in our setup because every gas particle is assumed to be comoving and thus is always away from the redshifted line center. j_ν of line sources in terms of the *comoving* luminosity density $\rho_c \equiv dL/dV_c = (1+z)^3 dL/dV$, with the comoving volume V_c and the emitted frequency ν_e , from sources at z is given by

$$j_{\nu_e}(z) = \frac{(1+z)^3 \rho_c(z)}{4\pi} \phi(\nu_e) = \frac{(1+z)^3 \rho_c(z)}{4\pi} \delta(\nu_e - \nu_0). \quad (10)$$

Using Eq.s (9) and (10) together with relations $\nu = \nu_e/(1+z)$ and $ds = dz c/[H(z)(1+z)]$, we obtain

$$I_\nu = \frac{c\rho_c(z)}{4\pi\nu_0 H(z)}, \quad (11)$$

where ν is now implicitly related to z as $\nu = \nu_0/(1+z)$.

Now we can address the dipole anisotropy of LIM using the conservation law $I'_{\nu'}/I_\nu = (\nu'/\nu)^3$ under the Lorentz transformation, or the Liouville theorem on the specific intensity (e.g. [21]). Using the Liouville theorem and Taylor-expanding I_ν in terms of quantities in ORF with the help of Eq. (2), we obtain

$$\frac{I'_{\nu',\text{dip}}}{I_{\nu'}} = \left(3 - \frac{\partial \ln I_\nu}{\partial \ln \nu} \Big|_{\nu'} \right) \beta = \left(3 + \frac{\partial \ln \rho_c}{\partial \ln(1+z)} \Big|_{z'} - \frac{\partial \ln H}{\partial \ln(1+z)} \Big|_{z'} \right) \beta. \quad (12)$$

Eq. (12) shows two aspects: (1) the first equality shows that the dipole of $I'_{\nu'}$ is determined by β and the the monopole $I_{\nu'}$ (amplitude and the spectral shape), and (2) the second equality shows a further dependence on cosmology through its dependence on the Hubble parameter. Even though the latter aspect seems attractive, using the dipole for probing H and its underlying parameters such as the matter content (Ω_m) and the dark energy equation of state ($\rho_{\text{DE}} \propto a^{-1(3+w)}$) can be obtained only when prior knowledge on $\rho_c(z')$ is established with the help of e.g. standard candles. Otherwise, we can only measure $I_{\nu'}$, and degeneracy between $\rho_c(z')$ and $H(z')$ is unavoidable for whichever cosmology we assume. $\rho_c(z')$ is to $I_{\nu'}$ what luminosity is to flux, and thus without a prior knowledge on the luminosity distance (D_L), $\rho_c(z')$ cannot be deduced from a sheer observation of $I'_{\nu',\text{dip}}/I_{\nu'}$. Diffuse LIMs do not have the luxury of hosting well-defined standard candles and are dominated by collection of lights from otherwise undetectable sources, and therefore the potential of using the LIM dipole for cosmology is slim.

Instead, the dipole of LIM can be used to perform astrophysics on large scales as follows. First, because there exist several independent estimates of $H(z')$, we can use these as a prior on $H(z')$ and then estimate β_\odot and the temporal evolution of ρ_c , or $\partial \ln \rho_c / \partial \ln(1+z)|_{z'}$, through observing $I'_{\nu',\text{dip}}/I_{\nu'}$. This information can then be linked to astrophysics such as the evolution of the star formation rate (e.g. Ly α LIM) or the amount of neutral gas (e.g. 21-cm LIM), etc. Second, under a given prior both on $H(z')$ and β_\odot , we could quantify the intrinsic dipole anisotropy or find a tension in the measure of β_\odot . Suppose that we first measure $\rho_c(z')$ through the measure of the monopole $I_{\nu'}$ and the prior on $H(z')$, using Eq. (11). Then, the measure of the dipole $I'_{\nu',\text{dip}}/I_{\nu'}$ should satisfy the last equality of Eq. (12), because all variables are constrained (ρ_c from the monopole measure, and H and β_\odot from the

prior). However, if the measure of the dipole $I'_{\nu',\text{dip}}/I_{\nu'}$ does not satisfy this equality, this means either the prior on β_{\odot} (e.g. from CMB dipole) is wrong or there exists an intrinsic dipole moment due to the inhomogeneous distribution of radiation sources projected as the anisotropy in the LIM. Relative motion of the matter-rest frame against the radiation-background-rest frame could be another resolution for such β_{\odot} tension.

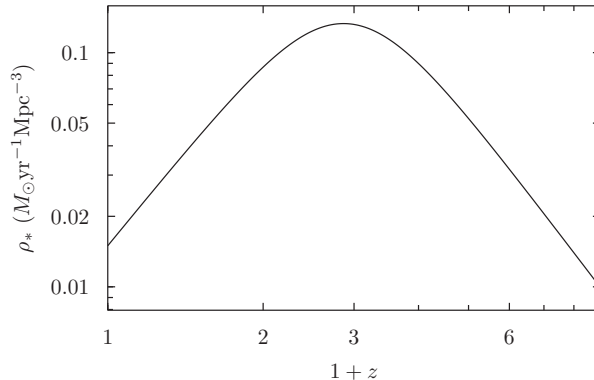


Fig. 1 Evolution of the star formation rate density shown as a fit (Eq. 14) to the observed data [23].

We adopt a parametric approach for inference. First, we assume a 3-parameter fit to the evolution of ρ_c such that

$$\frac{\partial \ln \rho_c}{\partial \ln(1+z)} = \gamma_1 - \frac{(\gamma_1 - \gamma_2)(1+z)^{\gamma_1 - \gamma_2}}{(1+z_t)^{\gamma_1 - \gamma_2} + (1+z)^{\gamma_1 - \gamma_2}}. \quad (13)$$

Eq. (13) is simply to test the power of the dipole measurement: the specific form used in Eq. (13) can sometimes pose a strong prior effect, in which case one can change the functional form into a more appropriate one if some hint on ρ_c is available. Nevertheless, Eq. (13) is based on the evolution of the star formation rate density (stellar mass generated per time and comoving volume) ρ_* at $z \lesssim 8$, well fit by the form

$$\rho_*(z) = \frac{2\rho_*(z_t)}{(1+z_t)^{\gamma_1}} \frac{(1+z)^{\gamma_1}}{1 + [(1+z)/(1+z_t)]^{\gamma_1 - \gamma_2}}. \quad (14)$$

ρ_* in this form peaks at $z \simeq z_t$, and roughly follows a broken power law: $\rho_*(z < z_t) \propto (1+z)^{\gamma_1}$ and $\rho_*(z > z_t) \propto (1+z)^{\gamma_2}$. The observed ρ_* is well fit by $\{\rho_*(z_t), z_t, \alpha, \beta\} \simeq \{0.133 M_{\odot} \text{yr}^{-1} \text{Mpc}^{-3}, 1.9, 2.7, -2.9\}$ in a wide redshift range, $z=0-8$ [23]. See Fig. 1 for this fit. If one assumes a constant mass-to-light ratio M/L , it is reasonable to let $\rho_c \propto \rho_*$ and thus we adopt Eq. (13) in this work. In order to accommodate the dependence of H on cosmological parameters when using a prior on cosmology, we use the fact that $\partial \ln H / \partial \ln(1+z) = \partial \ln E / \partial \ln(1+z)$ with

$$E(z) \equiv H(z)/H_0 = [\Omega_{m,0}(1+z) + \Omega_{k,0}(1+z)^2 + (1 - \Omega_{m,0} - \Omega_{k,0})f(z, w)], \quad (15)$$

where w is the dark energy equation of state,

$$f(z) = \exp\left(3 \int_0^z \frac{1+w(z'')}{1+z''} dz''\right) = (1+z)^{3(1+w_0+w_a)} \exp\left(-3w_a \frac{z}{1+z}\right), \quad (16)$$

and the last equality of Eq. (16) is valid only when one adopts the CPL (Chevallier-Polarski-Linder) parametrization of $w(z)$ [24, 25], namely

$$w(z) = w_0 + w_a \frac{z}{1+z}. \quad (17)$$

3 Forecasts

3.1 Galaxy number count

The dipole anisotropy in the galaxy number count is affected by the number of probed galaxies and the uncertainty in redshifts of a spectral line. The former and the latter restrictions mainly come from the telescope sensitivity and the spectral resolution, respectively. As the Poisson shot noise from a finite number of galaxies is one of the most severe restrictions, we focus only on $\mathcal{N}'(\nu', \hat{n})$ that could warrant the shot noise smaller than $n'(F', \nu', \hat{n}')$. The simple form of Eq. (8) allows an easy analytical assessment of the uncertainty at a frequency bin, by propagating errors,

$$\sigma_\beta(\nu') = \frac{\sqrt{\mathcal{N}'^2 \sigma_D^2 + D^2 \sigma_{\mathcal{N}'}^2}}{\mathcal{N}'^2 \left|1 - \frac{\partial \ln \mathcal{N}'}{\partial \ln \nu'}\right|_{\nu'}}, \quad (18)$$

where $\mathcal{N}' \equiv \mathcal{N}'(\nu')$, $D \equiv \mathcal{N}'_{\text{dip}}$ and σ_A is the standard deviation of a quantity A . Each uncertainty is inclusive of possible systematic uncertainties: e.g. $\sigma_{\mathcal{N}'} = (\mathcal{N}' + \sigma_{\text{ext}}^2)^{1/2}$ where $\mathcal{N}'^{1/2}$ is the Poisson shot noise and σ_{ext} is the uncertainty caused by the limited spectral resolution, etc.

Assuming an ideal case where the shot noise is the only cause of the uncertainties, one could estimate a most optimistic error (inverse of the signal-to-noise ratio) by letting $\sigma_{\mathcal{N}'} \simeq \sigma_D \simeq \mathcal{N}'^{1/2}$ in Eq. (18):

$$\begin{aligned} \frac{\sigma_\beta(\nu')}{\beta} &\simeq \frac{1}{\beta \sqrt{\mathcal{N}' \left|1 - \frac{\partial \ln \mathcal{N}'}{\partial \ln \nu'}\right|_{\nu'}}} \\ &\simeq 0.36 \left(\frac{\mathcal{N}'}{10^6}\right)^{-\frac{1}{2}} \left(\frac{\left|1 - \frac{\partial \ln \mathcal{N}'}{\partial \ln \nu'}\right|_{\nu'}}{5}\right)^{-\frac{1}{2}} \left(\frac{\beta}{1.23 \times 10^{-3}}\right)^{-1}. \end{aligned} \quad (19)$$

Eq. (19) already puts a severe constraint on a survey requirement. In order to obtain about $\leq 36\%$ error on each redshift bin, one needs to probe at least $\mathcal{N}' \geq 10^6$ galaxies per the redshift bin with the help of a steep spectral change in \mathcal{N}' , $\left|1 - \frac{\partial \ln \mathcal{N}'}{\partial \ln \nu'}\right|_{\nu'} \simeq 5$. In an unfortunate case with $\left|1 - \frac{\partial \ln \mathcal{N}'}{\partial \ln \nu'}\right|_{\nu'} \leq 1$, the error increases to $\geq 81\%$ with $\mathcal{N}' = 10^6$ or could remain at $\sim 36\%$ only when probing more galaxies, $\mathcal{N}' \simeq 2.3 \times 10^6$.

When there are N_z redshift bins, of course, the net error on σ_β/β will decrease to $\sim 1/N_z^{-1/2}$ of the bin-wise error, Eq. (19).

While demanding, such a requirement is within the easy reach of the SPHEREx survey that is scheduled to be launched around April 2025 and expected to probe 4.5×10^8 galaxies residing at $z = 0 - 2$ with spectroscopy. The existing full-sky galaxy surveys with photometry, such as WISE and 2MASS (Two Micron All Sky Survey) are too marginal to reliably use the spectral lines because (1) there are only 4 and 3 frequency bands in WISE and 2MASS, respectively, to filter a reliable spectroscopy and (2) the overall numbers of galaxies probed are only about 10^6 and 1.6×10^6 in WISE and 2MASS, respectively. Note that the dipole measurements using the WISE galaxies utilized not the line flux but the average continuum flux, which allowed the usage of the total number of galaxies ($\sim 10^6$) and allowed a $\sim 50\%$ error on estimating β at 1σ level. The spectroscopy-capable SPHEREx, combined with the largeness of the expected galaxy count, will enable a reliable measure of the dipole anisotropy. Nevertheless, even with SPHEREx the impact of the unavoidable mask on the galactic plane would not be trivial due to the leakage of other multipoles into the dipole and the shrinkage of the sky coverage, which should be carefully addressed in estimating the true dipole [26].

3.2 Line intensity mapping

There does not exist a full-sky LIM survey yet other than LIM surveys on limited regions of the sky, and therefore we perform a forecast on a possible future full-sky LIM survey. At the moment, intensive observational work is dedicated to the study of important spectral lines such as HI Ly α [27, 28], 21-cm [14, 16, 29], and CO lines [30, 31], but rather focusing on a limited target area of the sky. Therefore, we seriously suggest that low-angular resolution, large-angle LIM surveys be performed in the near future.

A full-sky LIM survey can be analyzed just by itself or in combination with other preexisting cosmological observations. Toward this, we perform a Fisher matrix analysis, using a MATLAB module "Fisher4Cast" developed by [32]. Fisher4Cast calculates the Fisher matrix

$$\begin{aligned} F_{AB} &= \sum_{\alpha} \left[\frac{\partial \mathbf{X}_{\alpha}^T}{\partial \theta_A} \mathbb{C}_{\alpha}^{-1} \frac{\partial \mathbf{X}_{\alpha}^T}{\partial \theta_B} + \frac{1}{2} \text{Tr} \left(\mathbb{C}_{\alpha}^{-1} \frac{\partial \mathbb{C}_{\alpha}}{\partial \theta_A} \mathbb{C}_{\alpha}^{-1} \frac{\partial \mathbb{C}_{\alpha}}{\partial \theta_B} \right) \right] \\ &= \sum_{\alpha} \sum_i \frac{1}{\sigma_{\alpha,i}^2} \frac{\partial X_{\alpha}(z_i)}{\partial \theta_A} \frac{\partial X_{\alpha}(z_i)}{\partial \theta_B}, \end{aligned} \quad (20)$$

where an observable \mathbf{X}_{α} is composed of multi-redshift probes at $\{z_i\}$ such that

$$\mathbf{X}_{\alpha} = (X_{\alpha}(z_1), X_{\alpha}(z_2), \dots, X_{\alpha}(z_n)), \quad (21)$$

\mathbb{C}_{α} is the covariance matrix of observable X_{α} such that $(\mathbb{C}_{\alpha})_{ij} \equiv \langle (X_{\alpha}(z_i) - \langle X_{\alpha}(z_i) \rangle)(X_{\alpha}(z_j) - \langle X_{\alpha}(z_j) \rangle) \rangle$, and θ_i denotes underlying parameters: energy contents ($\Omega_{m,0}$ and $\Omega_{k,0}$), equation of state parameters (w_0 and w_a), the current-day Hubble

constant H_0 , the solar velocity against the background-rest frame β_\odot , and the astrophysical parameters γ_1 , γ_2 , and z_t . The last equality in Eq. (20) is usually used, which is in principle valid only when measurement errors are independent of cosmological parameters and across observing redshifts. We follow this convention in this work. When to apply a prior information on θ_i , a diagonal matrix $P_{AB} = \delta_{AB}/\sigma_A^2$ is added to F_{AB} to form a new Fisher matrix, where δ is the Kronecker delta and σ_A is the standard deviation of θ_A obtained through pre-existing observations. We limit our observables to $X = \{H, D_A, I'_{\nu', \text{dip}}/I_{\nu'}\}$ where H is the Hubble coefficient, D_A is the angular diameter distance, and $I'_{\nu', \text{dip}}/I_{\nu'}$ is the ratio of the dipole to the monopole of a LIM. We only consider (1) the combination of all of H , D_A and LIM and (2) the LIM-only observation but with priors on cosmological parameters.

3.2.1 Case 1: Combined observation of H , D_A and $I'_{\nu', \text{dip}}/I_{\nu'}$

We present our forecast on a combined observation of H , D_A and $I'_{\nu', \text{dip}}/I_{\nu'}$. Measuring H and D_A allows estimation of cosmological parameters. We assume an almost ideal situation, where we have only 1% error³ on both H and D_A at each of the 20 redshift bins equally spaced at $z=[0, 2]$, and 3% error on $I'_{\nu', \text{dip}}/I_{\nu'}$ at each of the 40 redshift bins equally spaced at $z=[0, 4]$. The reason to stretch the redshift range of $I'_{\nu', \text{dip}}/I_{\nu'}$ is to include both the increasing and decreasing trends in ρ_c at $z > z_t \simeq 2$ and $z < z_t \simeq 2$, respectively. If the redshift range of $z \gtrsim 2$ were excluded but ρ_c followed the form of Eq. (14), then γ_2 would not be constrained.

Having such an accurate measurement of H and D_A would allow a reliable estimation of not only the cosmological parameters but also β_\odot , γ_1 , γ_2 , and z_t . In the light of the recent measures of the baryon acoustic oscillation (BAO) [33] and an Alcock-Paczynski test [34] hinting at non-standard cosmology with $w_0 \neq 1$ and $w_a \neq 0$, we just include these parameters to have a triangle plot on marginalized posterior distributions in Fig. 2. Through the help of accurate measures of H and D_A , our Fisher matrix analysis results in the marginalized 1D estimations shown in Table 1. Marginalized 2D posterior contours of 1σ and 2σ confidence levels are shown in Fig. 2.

Table 1 Parameter-estimation potential of two observational strategies (Sects. 3.2.1 and 3.2.2), expressed in terms of per-cent error in each parameter.

parameters θ	w_0	w_a	β_\odot	γ_1	γ_2	z_t
fiducial values	-0.727	-1.05	0.00123	2.7	-2.9	1.9
1σ % error for $H+D_A + I'_{\nu', \text{dip}}/I_{\nu'}$	8.7	35	1.9	2.8	0.7	0.5
1σ % error for $I'_{\nu', \text{dip}}/I_{\nu'} + (\text{cosmological priors})$	(9.2) ¹	(28)	9.7	12	2.5	2.8

The per-cent errors are based on the fiducial values listed.

¹Numbers in parentheses are priors.

³We assume such a high accuracy on measures of H and D_A in order to achieve a marginalized posterior on w_0 comparable to the accuracy reported by a recent Alcock-Paczynski test [34]. This test uses seemingly anisotropic clustering of galaxies and thus it is not straightforward to translate its accuracy to the measures of H and D_A . Instead, we tried several values of the observational accuracy in H and D_A and found that the quoted accuracy leads to $\sim 9\%$ error on the marginalized estimation of w_0 . One may accept this choice as a reflection of the combined power of various cosmological observations.

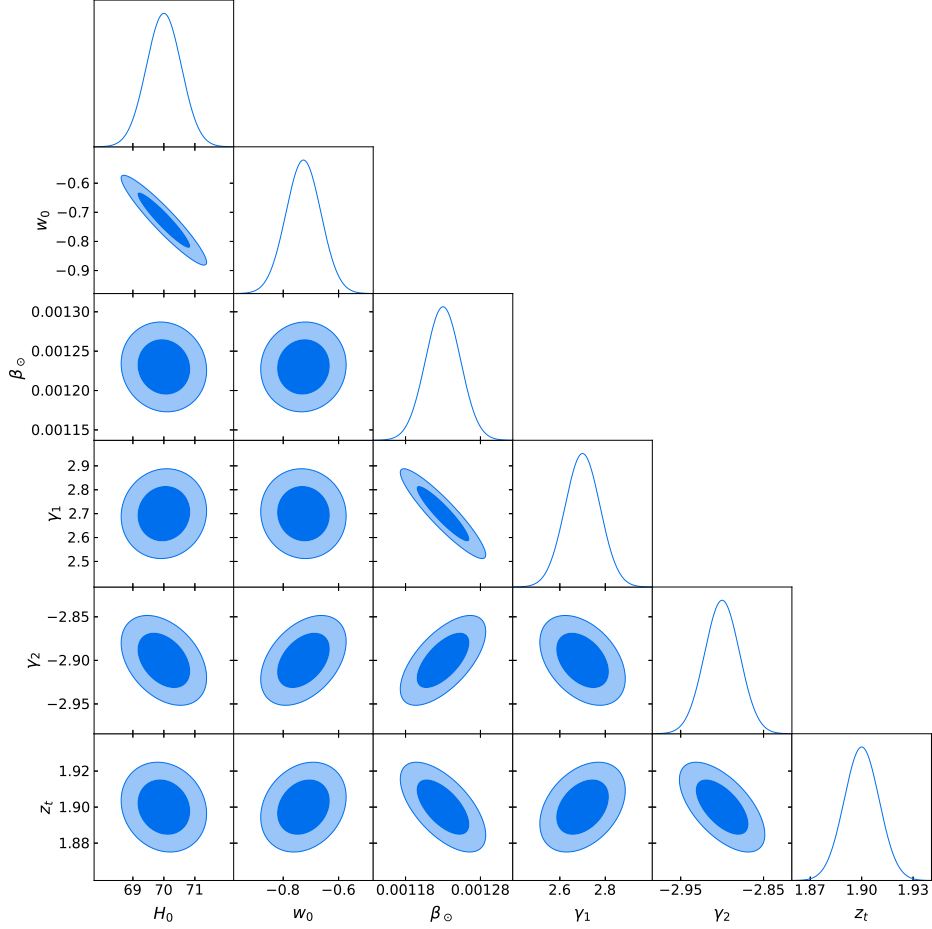


Fig. 2 Forecast for an ideal $H+D_A + I'_{\nu',dip}/I_{\nu'}$ observation, assuming 1% error on H and D_A at each of 40 redshift bins from $z=0$ to 2 and 3% error on $I'_{\nu',dip}/I_{\nu'}$ at each of 40 redshift bins from $z=0$ to 4. Expected estimation of parameters H_0 , w_0 , β_{\odot} , γ_1 , γ_2 , and z_t after marginalization over other cosmological parameters. Shown are 2D contours of 1σ and 2σ confidence levels, and the 1D posterior distributions.

3.2.2 Case 2: Dipole-only measurement with priors on cosmological parameters

We now forecast a fractional dipole measurement of LIM, $I'_{\nu',dip}/I_{\nu'}$, combined with priors on cosmological parameters from pre-existing observations. The priors we use here are $H_0 = (70 \pm 1.1) \text{ km s}^{-1} \text{ Mpc}^{-1}$, $\Omega_{m,0} = 0.3 \pm 0.023$, $\Omega_{k,0} = 0 \pm 0.002$ [35], $w_0 = -0.727 \pm 0.67$, and $w_a = -1.05 \pm 0.29$ [33]. We do not here encompass the "Hubble tension" between the estimations from the CMB observation and the measurement of relatively local standard candles, but instead just adopt the estimation from the latter. We then assume an observation of $I'_{\nu',dip}/I_{\nu'}$ that has the observational error of 10% at each of 20 uniformly spaced redshift bins at $z=[0, 4]$.

The result is still promising as shown in Table 1 and Fig. 3, even though the error budgets increase to ~ 5 times those of the combined observation (Sect. 3.2.1). All parameters are found to be with estimation error $\lesssim 10\%$, and especially β_{\odot} with 9.7% error. Table 1 and Fig. 3 shows the result. This result shows that the dipole-only measurement can constrain both β_{\odot} and the temporal evolution of ρ_c , thus providing a valuable information on astrophysics.

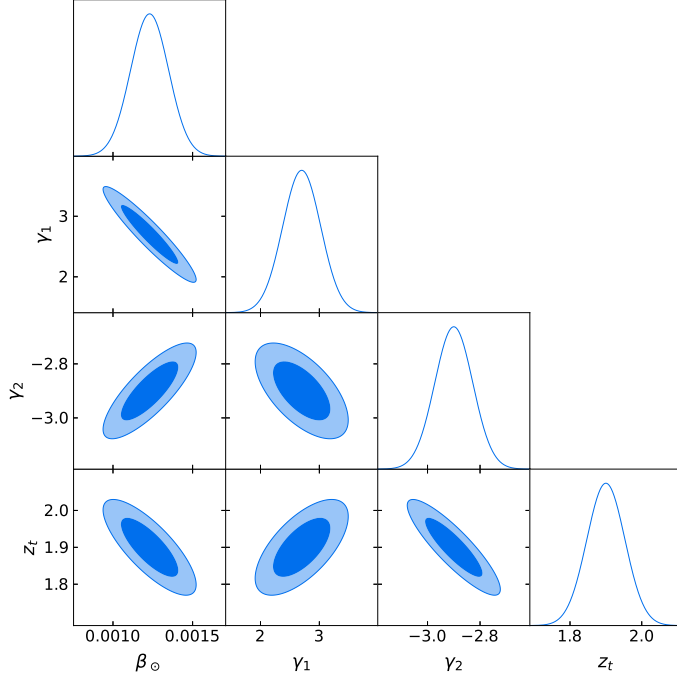


Fig. 3 Forecast for an $I'_{\nu', \text{dip}}/I_{\nu'}$ -only observation at 10% error at each of 40 redshift bins from $z=0$ to 4 with priors on cosmological parameters.

4 Summary and Discussion

Spectral-line based mapping of galaxies or diffuse intensities can reveal the dipole anisotropy due to the motion of our solar system. These SGS and LIM dipoles are separated in frequencies, or equivalently in redshifts of origin, and thus provide natural redundancy in the estimation of the dipole. Therefore, we expect that such surveys could provide a reliable constraint on β_{\odot} . Full-sky SGS such as the upcoming SPHEREx allows a luxurious number of galaxies large enough to provide an excellent constraint on β_{\odot} . As for LIM, there does not exist a full-sky LIM yet proposed. There exist some existing or planned telescopes with the spectroscopic capability and the sky coverage of about 50 – 70%, e.g. 21-cm line survey instrument SKA-LOW, which may be used for the LIM dipole measurement if a pattern-matching scheme is adopted

to overcome the limitation of the incomplete sky coverage [6]. In this work, we simulated the usage of a future full-sky LIM survey data. Such an observation, combined with already-existing prior constraints on cosmological parameters, is found to be able to place strong constraints on astrophysical parameters as well as β_{\odot} . Such surveys would not require a high angular resolution, and thus we propose a low angular resolution LIM survey that would observe the sky with a high speed. We defer setting up a more detailed observational strategy to a future paper.

We now discuss, for serendipity, a fictitious case where the estimated β_{\odot} from either the SGS dipole or the LIM dipole is found very different from the CMB-dipole based constraint, $\beta_{\odot, \text{CMB}} = (1.23 \pm 0.017) \times 10^{-3}$. Such a result can further be categorized into (1) the one with the directional consistency and (2) the one with the directional inconsistency. First, if there exists directional consistency, then there seems to be only two possibilities: (a) the galaxy bias is strong enough to contribute an additional dipole moment but galaxies still probe the local structure that causes the motion of the solar system against the CMB-rest frame, or (b) there exists a systematic uncertainty in observation. Second, if there exists directional inconsistency, the possibilities are (a) CMB-rest and matter-rest frames are moving against each other, or (b) there again exists a systematic uncertainty in observation. It is easy to blame the systematic uncertainties, but the evidences for strong discrepancies seem to be piling up.

What if our local universe within $\lesssim 3$ Gpc were statistically peculiar? There exist such symptoms indeed, and most notable one is the discrepancy between the measures of the baryon acoustic oscillation signature in the northern and southern Galactic caps [36]. Even though this fact is usually ignored and attributed again to observation-based uncertainties, it is interesting to take it as a true peculiarity of our local universe and find its possible link to the dipole discrepancy. The most natural way to link this north-south tension would be to have the local matter-rest frame moving against the CMB-rest frame, or simply having an additional effect on the dipole from the local inhomogeneity of matter distribution. Now, the launch of SPHEREx is imminent and thus the dipole anisotropy of the SGS by SPHEREx, in a number large enough to provide us with a tight constraint on β_{\odot} , is thus highly anticipated and would either deepen or simply resolve the puzzle. We also argue that it is good time to seriously consider full-sky LIM surveys for the same reason. Such surveys will provide a deep insight into the present day cosmology that tends to lean toward a possible non-standard cosmology other than the Λ CDM model.

Acknowledgements. KA is supported by NRF-2021R1A2C1095136 and a research grant from Chosun University (2017). KA also acknowledges the hospitality of Curtin University, where part of this work was conducted.

References

- [1] Yasini, S., Pierpaoli, E.: Beyond the boost: Measuring the intrinsic dipole of the cosmic microwave background using the spectral distortions of the monopole and quadrupole. *Phys. Rev. Lett.* **119**(22), 221102 (2017) <https://doi.org/10.1103/PhysRevLett.119.221102>

- [2] Ellis, G.F.R., Baldwin, J.E.: On the expected anisotropy of radio source counts. *Mon. Not. R. Astron. Soc.* **206**, 377–381 (1984) <https://doi.org/10.1093/mnras/206.2.377>
- [3] Xia, J.-Q., Viel, M., Baccigalupi, C., De Zotti, G., Matarrese, S., Verde, L.: Primordial Non-Gaussianity and the NRAO VLA Sky Survey. *Astrophys. J. Lett.* **717**(1), 17–21 (2010) <https://doi.org/10.1088/2041-8205/717/1/L17>
- [4] Singal, A.K.: Large peculiar motion of the solar system from the dipole anisotropy in sky brightness due to distant radio sources. *Astrophys. J.* **742**(2), 23 (2011) <https://doi.org/10.1088/2041-8205/742/2/123>
- [5] Chen, S., Schwarz, D.J.: Angular two-point correlation of NVSS galaxies revisited. *Astron. Astrophys.* **591**, 135 (2016) <https://doi.org/10.1051/0004-6361/201526956>
- [6] Secrest, N.J., von Hausegger, S., Rameez, M., Mohayaee, R., Sarkar, S., Colin, J.: A Test of the Cosmological Principle with Quasars. *Astrophys. J. Lett.* **908**(2), 51 (2021) <https://doi.org/10.3847/2041-8213/abdd40>
- [7] Dalang, C., Bonvin, C.: On the kinematic cosmic dipole tension. *Mon. Not. R. Astron. Soc.* **512**(3), 3895–3905 (2022) <https://doi.org/10.1093/mnras/stac726>
- [8] Kumar Aluri, P., Cea, P., Chingangbam, P., Chu, M.-C., Clowes, R.G., Hutsemékers, D., Kochappan, J.P., Lopez, A.M., Liu, L., Martens, N.C.M. et al.: Is the observable universe consistent with the cosmological principle? *Class. Quantum Gravity* **40**(9), 094001 (2023) <https://doi.org/10.1088/1361-6382/acbefc>
- [9] Darling, J.: The universe is brighter in the direction of our motion: Galaxy counts and fluxes are consistent with the cmb dipole. *Astrophys. J. Lett.* **931**(2), 14 (2022) <https://doi.org/10.3847/2041-8213/ac6f08>
- [10] Panwar, M., Jain, P., Omar, A.: Colour dependence of dipole in catwise2020 data. *Mon. Not. R. Astron. Soc. Lett.* **535**(1), 63–69 (2024) <https://doi.org/10.1093/mnrasl/slae093>
- [11] Tiwari, P., Nusser, A.: Revisiting the nvss number count dipole. *J. Cosmol. Astropart. Phys.* **2016**(03), 062–062 (2016) <https://doi.org/10.1088/1475-7516/2016/03/062>
- [12] Domènech, G., Mohayaee, R., Patil, S.P., Sarkar, S.: Galaxy number-count dipole and superhorizon fluctuations. *Journal of Cosmology and Astroparticle Physics* **2022**(10), 019 (2022) <https://doi.org/10.1088/1475-7516/2022/10/019>
- [13] Crill, B.P., Werner, M., Akeson, R., Ashby, M., Bleem, L., Bock, J.J., Bryan, S., Burnham, J., Byunh, J., Chang, T.-C. et al.: Spherex: Nasa’s near-infrared spectrophotometric all-sky survey. In: Lystrup, M., Perrin, M.D. (eds.) *Space*

Telescopes and Instrumentation 2020: Optical, Infrared, and Millimeter Wave. Society of Photo-Optical Instrumentation Engineers (SPIE) Conference Series, vol. 11443, p. 114430 (2020). <https://doi.org/10.1117/12.2567224> .

- [14] Mertens, F.G., Mevius, M., Koopmans, L.V.E., Offringa, A.R., Mellema, G., Zaroubi, S., Brentjens, M.A., Gan, H., Gehlot, B.K., Pandey, V.N. et al.: Improved upper limits on the 21 cm signal power spectrum of neutral hydrogen at $z \approx 9.1$ from lofar. *Mon. Not. R. Astron. Soc.* **493**(2), 1662–1685 (2020) <https://doi.org/10.1093/mnras/staa327>
- [15] Ahn, K., Mesinger, A., Alvarez, M.A., Chen, X.: Probing the first galaxies and their impact on the intergalactic medium through 21-cm observations of the cosmic dawn with the ska. In: *Advancing Astrophysics with the Square Kilometre Array (AASKA14)*, p. 3 (2015). <https://doi.org/10.22323/1.215.0003> .
- [16] Labate, M.G., Waterson, M., Alachkar, B., Hendre, A., Lewis, P., Bartolini, M., Dewdney, P.: Highlights of the square kilometre array low frequency (ska-low) telescope. *J. Astron. Telesc. Instrum. Syst.* **8**(01) (2022) <https://doi.org/10.1117/1.jatis.8.1.011024>
- [17] Hotinli, S.C., Ahn, K.: Probing the global 21 cm background by velocity-induced dipole and quadrupole anisotropies. *Astrophys. J.* **964**(1), 21 (2024) <https://doi.org/10.3847/1538-4357/ad2209>
- [18] Ahn, K., Oh, M.: Probing the global 21-cm signal via the integrated sachs-wolfe effect on the 21-cm background. *Phys. Rev. D* **109**(4), 043539 (2024) <https://doi.org/10.1103/PhysRevD.109.043539>
- [19] Bottani, S., Bernardis, P., Melchiorri, F.: On the origin of the dipole anisotropy as determined by quadrupole measurements. *Astrophys. J. Lett.* **384**, 1 (1992) <https://doi.org/10.1086/186250>
- [20] Challinor, A., van Leeuwen, F.: Peculiar velocity effects in high-resolution microwave background experiments. *Phys. Rev. D* **65**(10), 103001 (2002) <https://doi.org/10.1103/PhysRevD.65.103001>
- [21] Rybicki, G.B., Lightman, A.P.: *Radiative Processes in Astrophysics* (1979)
- [22] Peacock, J.A.: *Cosmological Physics* (1999).
- [23] Madau, P., Dickinson, M.: Cosmic star-formation history. *Annu. Rev. Astron. Astrophys.* **52**, 415–486 (2014) <https://doi.org/10.1146/annurev-astro-081811-125615>
- [24] Chevallier, M., Polarski, D.: Accelerating Universes with Scaling Dark Matter. *International Journal of Modern Physics D* **10**(2), 213–223 (2001) <https://doi.org/10.1142/S0218271801000822>

- [25] Linder, E.V.: Exploring the Expansion History of the Universe. *Phys. Rev. Lett.* **90**(9), 091301 (2003) <https://doi.org/10.1103/PhysRevLett.90.091301>
- [26] Abghari, A., Bunn, E.F., Hergt, L.T., Li, B., Scott, D., Sullivan, R.M., Wei, D.: Reassessment of the dipole in the distribution of quasars on the sky. *arXiv e-prints*, 2405.09762 (2024) <https://doi.org/10.48550/arXiv.2405.09762>
- [27] Östlin, G., Hayes, M., Duval, F., Sandberg, A., Rivera-Thorsen, T., Marquart, T., Orlitová, I., Adamo, A., Melinder, J., Guaita, L. et al.: The $\text{Ly}\alpha$ reference sample. i. survey outline and first results for markarian 259. *Astrophys. J.* **797**(1), 11 (2014) <https://doi.org/10.1088/0004-637X/797/1/11>
- [28] Ahumada, R., Allende Prieto, C., Almeida, A., Anders, F., Anderson, S.F., Andrews, B.H., Anguiano, B., Arcodia, R., Armengaud, E., Aubert, M. et al.: The 16th data release of the sloan digital sky surveys: First release from the apogee-2 southern survey and full release of eboss spectra. *Astrophys. J. Suppl. Ser.* **249**(1), 3 (2020) <https://doi.org/10.3847/1538-4365/ab929e>
- [29] HERA Collaboration, Abdurashidova, Z., Adams, T., Aguirre, J.E., Alexander, P., Ali, Z.S., Baartman, R., Balfour, Y., Barkana, R., Beardsley, A.P. et al.: Improved constraints on the 21 cm eor power spectrum and the x-ray heating of the igm with hera phase i observations. *Astrophys. J.* **945**(2), 124 (2023) <https://doi.org/10.3847/1538-4357/acaf50>
- [30] Keating, G.K., Marrone, D.P., Bower, G.C., Leitch, E., Carlstrom, J.E., DeBoer, D.R.: Copss ii: The molecular gas content of ten million cubic megaparsecs at redshift $z \sim 3$. *Astrophys. J.* **830**(1), 34 (2016) <https://doi.org/10.3847/0004-637X/830/1/34>
- [31] Li, T.Y., Wechsler, R.H., Devaraj, K., Church, S.E.: Connecting co intensity mapping to molecular gas and star formation in the epoch of galaxy assembly. *Astrophys. J.* **817**(2), 169 (2016) <https://doi.org/10.3847/0004-637X/817/2/169>
- [32] Bassett, B.A., Fantaye, Y., Hlozek, R., Kotze, J.: Fisher matrix preloaded — fisher4cast. *Int. J. Mod. Phys. D* **20**(13), 2559–2598 (2011) <https://doi.org/10.1142/S0218271811020548>
- [33] DESI Collaboration, Adame, A.G., Aguilar, J., Ahlen, S., Alam, S., Alexander, D.M., Alvarez, M., Alves, O., Anand, A., Andrade, U. et al.: DESI 2024 VI: Cosmological Constraints from the Measurements of Baryon Acoustic Oscillations. *arXiv e-prints*, 2404–03002 (2024) <https://doi.org/10.48550/arXiv.2404.03002>
- [34] Dong, F., Park, C., Hong, S.E., Kim, J., Hwang, H.S., Park, H., Appleby, S.: Tomographic Alcock-Paczyński Test with Redshift-space Correlation Function: Evidence for the Dark Energy Equation-of-state Parameter $w > -1$. *Astrophys. J.* **953**(1), 98 (2023) <https://doi.org/10.3847/1538-4357/acd185>

- [35] Planck Collaboration, Aghanim, N., Akrami, Y., Ashdown, M., Aumont, J., Baccigalupi, C., Ballardini, M., Banday, A.J., Barreiro, R.B., Bartolo, N. et al.: Planck 2018 results. vi. cosmological parameters. *Astron. Astrophys.* **641**, 6 (2020) <https://doi.org/10.1051/0004-6361/201833910> arXiv:1807.06209 [astro-ph.CO]
- [36] Tojeiro, R., Ross, A.J., Burden, A., Samushia, L., Manera, M., Percival, W.J., Beutler, F., Brinkmann, J., Brownstein, J.R., Cuesta, A.J. et al.: The clustering of galaxies in the sdss-iii baryon oscillation spectroscopic survey: galaxy clustering measurements in the low-redshift sample of data release 11. *Mon. Not. R. Astron. Soc.* **440**(3), 2222–2237 (2014) <https://doi.org/10.1093/mnras/stu371>